Iranian Journal of Science & Technology, Transaction A, Vol. 33, No. A1
Printed in the Islamic Republic of Iran, 2009

IONIZATION OF A 1-D MODEL OF H_2^+ FROM DIFFERENT STATES IN INTENSE LASER FIELD*

H. SABZYAN** AND H. EBADI

Department of Chemistry, University of Isfahan, Isfahan 81746-73441, I. R. Iran
Email: sabzyan@sci.ui.ac.ir

Abstract – Time-dependent Schrödinger equation for a 1-D model of hydrogen molecular ion H_2^+ in intense laser field linearly polarized along the molecular axis is solved. Ionization rates are calculated for different initial states. The evolution of electronic wavefunction at fixed inter-nuclear separations are simulated and analyzed. The results obtained for the ground state of this 1-D model of H_2^+ show appreciable qualitative agreement with the results obtained previously in the 2-D and 3-D studies. The Ponderomotive energy effect on the beginning of ionization in different initial states is observed. The above threshold ionization has a large contribution in the ionization of electrons, except for the ground state and at equilibrium inter-nuclear separation. The ionization rates show that at some inter-nuclear separations larger than 4.0 *au*, resonance enhancement ionization by some higher excited states occur. At inter-nuclear separations shorter than 4.0 *au*, the ground state does not show any resonance with higher excited states.

Keywords – Intense laser; TDSE; above threshold, ionization rate; H_2^+; Ponderomotive; wavepacket; 1-D model

1. INTRODUCTION

In the past two decades, a number of interesting phenomena related to the interaction of atoms and molecules with short laser pulses have been observed and studied [1]. In the simple case, these phenomena arise from the interaction of the electrons of an atom with a strong laser field. This interaction may result in the ionization of an electron and its acceleration, and possibly recombination with the parent atom or molecule to generate a high energy XUV photon (high harmonic generation) [2, 3]. Recollision of the (free) ionized electron with the parent molecule has an important role in the pattern of fragmentation and its further ionization steps. For example, the ionized electron from the H_2^+ molecule is driven back by the laser field to collide with the H_2^+ ion, which may result in the second ionization or excitation of the H_2^+ ion. The excited H_2^+ ion can then be dissociated directly, or ionized by the laser field [4-7].

Theoretical studies in this field are based on the dipole approximation for laser-atom interactions. Such an approximation is valid for laser intensities that are not high enough to accelerate the electrons to relativistic velocities.

In the intense laser field, photoelectron spectra show many peaks corresponding to the absorption of more photons than the minimum number necessary for ionization. The phenomena in which an electron is ionized by a number of photons more than needed to increase electron energy up to ionization potential is called above-threshold ionization or simply ATI [8]. The energies of dissociating molecular fragments also show absorption or emission of additional photons beyond the minimum order process. This phenomena is called above-threshold dissociation and acronymed ATD [9]. In intense laser field, these two phenomena compete.

*Received by the editor May 22, 2007 and in final revised form November 2, 2009
**Corresponding author

When the laser intensity is above ~10^{14} W/cm^2 (corresponding to a peak electric field of ≈1 V/Å via $I = \frac{1}{2} c \varepsilon_0 E_0^2$), the light induced shift in the energies of molecular states becomes quite large, often larger than the photon energy $\hbar\omega$. Ordinary perturbation theory is not very useful for calculating absorption rates in this intensity regime, as many of the photons may be absorbed during a single dissociation or ionization process.

The extra energy induced by the laser field on a weakly bound electron is comparable to a classical quantity known as the *ponderomotive potential*. This potential, which is the cycle-averaged kinetic energy of a free electron wiggling in an oscillating electromagnetic field, is given by [10]:

$$U_P = \frac{e^2 E_0^2}{4m\omega^2} \tag{1}$$

in which m is the mass of electron at rest, e is its charge, E_0 is the peak electric field and ω is the frequency of the laser pulse. The ponderomotive energy increases quadratically with wavelength, and is linear in intensity (intensity quadratically depends on the peak electric field). For example, for the intensity of 10^{13} W/cm^2 and λ=1.06 μm, U_P is about 1 eV. The light-induced shifts in the levels of a molecule can be comparable to U_P, and therefore should be directly observable in photoelectron spectra. Although the source of this energy is kinetic, it acts like an effective potential energy. A charged particle in an inhomogeneous region of intensity, such as that in a laser focus, experiences a time-averaged force equal to the negative gradient of this ponderomotive potential. In the weakly bound Rydberg states, the ponderomotive contribution dominates, while in the ground state, ponderomotive motion and bound state couplings tend to cancel [11].

In time-dependent quantum mechanics, the wavefunction $\Psi(\vec{r}, t)$ at time t is obtained by solving the time-dependent Schrödinger equation (TDSE). This is accomplished numerically in what is called the grid method, by representing the initial state of the system by $\Psi(\vec{r}, 0)$ on a discrete grid in coordinate space, and following its evolution by slicing time into small intervals [1-3, 8]. The nature of the laser field requires the use of a time-dependent vector potential scheme for the laser-atom and laser-molecule interactions in the Hamiltonian of the system [1-3].

Over the past decade, powerful computational hardware and software facilities have allowed the numerical solution of the 1-D and 2-D TDSE, and attempts towards the solution of the full dimensional H_2^+, including electronic and nuclear dynamics, has been in order in this field of physics. Results of these studies effectively describe the phenomena of the interaction of short pulse lasers with atoms and molecules [12-15]. In spite of limitations in the description of the 3-D actual system, the unrealistic 1-D model is a useful starting point for the study of different phenomena and preliminary evaluation of new approaches and numerical methods proposed for the study of 3-D systems in a reasonable amount of time. Results of the 1-D model can thus be used for a qualitative description of the system behavior. Application of the 1-D model for the atom-laser interaction was examined first by Geltman [16, 17]. In a 1-D simple model, some selections of parameters, such as magnetic field and circular polarization (of the laser field) are essentially neglected. Since one-dimensional calculation is fast, the effects of a variety of parameters such as pulse length and large spatial grids can be investigated. A 1-D model is adopted in order to see how the picture of the physical details of the system is distorted and what part of the phenomena are expressed correctly (at least qualitatively) when reducing the dimensionality of the system. The results obtained from the 1-D model studies are important in that they can serve as a guide in the future studies on the 2-D and 3-D atom-laser or molecule-laser interactions. Success and feasibility of the application of new methods, and the study with new laser field intensities and/or under different system conditions can be tested on the 1-D model prior to the calculations on the actual system.

In this work, TDSE describing the interaction of the 1-D model of the H_2^+molecule in different initial states with an intense linearly polarized laser field is solved numerically using available efficient numerical methods [18-21]. A real space-time evolution approach based on Suzuki's fractal decomposition with the Cayley form [22] has been used. Orthonormality and overall norm (i.e. sum of the ionized and the remained parts of the norm of the wavepacket) of the system are preserved during all steps of the calculations. An adaptive grid [12-15] is used for the discretization of the only coordinate of the 1-D space. Ionization rates of this 1-D model molecular system from different initial states are then calculated for different inter-nuclear separations.

2. COMPUTATIONAL MODEL

There is a range of laser parameters (frequency and intensity) at which the velocity of the electron is small enough to permit the assumption that the electron dynamics is described by the Schrödinger equation and large enough to include the first-order relativistic corrections. In this region, TDSE with scalar potential, $V(\vec{r}\,)$, and time-dependent vector potential, $\vec{A}(\vec{r},t)$, has the following form in atomic units (e=1, m_e=1, $\hbar$=1, c=137):

$$i\frac{\partial\Psi(\vec{r},t)}{\partial t}=\left[\frac{1}{2}\left(-i\vec{\nabla}-\frac{1}{c}\vec{A}(\vec{r},t)\right)^2+V(\vec{r})\right]\Psi(\vec{r},t) \tag{2}$$

For the linear molecule H_2^+, the soft-core scalar Coulomb potential in the x direction is:

$$V(x)=-\frac{1}{((x-R/2)^2+a)^{1/2}}-\frac{1}{((x+R/2)^2+a)^{1/2}} \tag{3}$$

in which a is a parameter that allows avoiding singularities at the origins and is chosen to be a=1.52 in our calculations to produce the energy eigenvalue of our interest in the absence of the laser field. Increasing the value of a results in a flatter potential and a higher energy for the 1-D model of H_2^+, and consequently, in a more spread out initial wavepacket. The spatial adaptive (non-uniform) grid used in these calculations has 570 points. In this grid, and for the chosen value of a, the ground state of the 1-D model molecule has an energy of E_g = −0.59, as determined by the standard imaginary-time propagation method. The excited states of the H_2^+ molecule are determined numerically using imaginary time Gram-Schmitt orthogonalization method. Polarization and the wave vector of the laser pulse are assumed to be along the x and y axes, respectively. The space dependence of the field has been neglected and dipole approximation is assumed. Therefore, the monochromatic electric field applied on the H_2^+ molecular ion takes the form:

$$E_x(t)=E_{0x}f(t)\cos(\omega t) \tag{4}$$

in which E_{0x} is the maximum strength of the electric field of the laser pulse, ω is angular frequency, $f(t)$ is an envelope function with a ramp-on from 0 to 1 during $0\le t<t_1$, then becoming constant, 1, from t_1 to t_2 and then ramped-off to 0 during $t_2<t\le t_3$; t_3 is thus the overall duration of the pulse. We have used the following form for the envelope of the laser field:

$$f(t)=\begin{cases} \frac{1}{2}\left[\left(1-\cos\left(\frac{\pi t}{t_1}\right)\right)\right] & 0 \le t < t_1 \\ 1 & t_1 \le t \le t_2 \\ \frac{1}{2}\left[1+\cos\left(\frac{\pi(t-t_2)}{(t_3-t_2)}\right)\right] & t_2 < t \le t_3 \\ 0 & t_3 < t \end{cases} \tag{5}$$

In our study, t_1, t_2 and t_3 are chosen to be four, fourteen and eighteen periods of the laser pulse, respectively.

The vector potential $\vec{A}(\vec{r},t)$ in Eq. (2), denoted simply by $A_x(t)$ in the 1-D space within the long wavelength approximation, is defined by

$$A_x(t)=-c\int_0^t E_x(t')dt' \tag{6}$$

in which $E_x(t')$ is given by Eq. (4) and c is the speed of light.

One serious problem in time-dependent quantum mechanical calculations is that, as time progresses, the wave packet (WP) reaches the grid edges and undergoes spurious reflections or wraps around, depending on the type of method used in evaluating the action of the kinetic energy operator on $\Psi(\vec{r},t)$. One way to avoid this problem is to use a very large grid which would delay the WP reaching the boundaries. This would mean a tremendous increase in the allocated computer memory and the calculation time which is not feasible in many practical applications. Thus, to avoid these difficulties a negative imaginary potential (NIP) is used. When the NIPs are added to the Hamiltonian, WP is absorbed near the boundaries. For the one-dimensional system of our interest, in the presence of the laser field and NIP, the TDSE now takes the form:

$$i\frac{\partial}{\partial t}\Psi(x,t)=\left[-\frac{1}{2}\left(\frac{\partial^2}{\partial x^2}\right)-\frac{i}{c}A_x(t)\frac{\partial}{\partial x}+V(x)+V_I(x)\right]\Psi(x,t) \tag{7}$$

in which $V(x)$ and $A_x(t)$ are given respectively by Eqs. (3) and (6). The NIP set on the borders of the grid box acts as an absorbing wall [23]. We have chosen the following form for $V_I(x)$.

$$V_I(x)=\begin{cases} -iV_o\left[\frac{x-x_1}{x_2-x_1}\right]^{\alpha} & x_1 \le x \le x_2 \\ 0 & \text{otherwise} \end{cases} \tag{8}$$

Here, x_1 and x_2 define the range in which the NIP is operative. In our calculation, V_o and α parameters adjusting the NIP variation are set to 5.0 and 4.0, respectively.

In the split operator (SO) method used in the present study, the wave function at time $t+\Delta t$ is calculated from the wave function at the previous time step t using:

$$\Psi(x,\Delta t)=\exp\left\{\left[\frac{i}{2}\left(\frac{\partial^2}{\partial x^2}\right)-\frac{1}{c}A_x(t)\frac{\partial}{\partial x}-iV(x)-iV_I(x)\right]\Delta t\right\}\Psi(x,t)$$

$$\cong\exp\left[i\frac{\Delta t}{2}\left(\frac{1}{2}\frac{\partial^2}{\partial x^2}\right)\right]\exp\left[-i\Delta t\left(V_I(x)+V(x)-\frac{i}{c}A_x(t)\frac{\partial}{\partial x}\right)\right]\exp\left[i\frac{\Delta t}{2}\left(\frac{1}{2}\frac{\partial^2}{\partial x^2}\right)\right]\Psi(x,t) \qquad (9)$$

which is evaluated using Crank-Nicholson finite-difference scheme. The SO scheme, even in the presence of NIP, is unconditionally stable. It conserves norm but does not conserve energy.

The ionization rate Γ is related to the initial and instantaneous norm of the system, $|\Psi(0)|^2$ and $|\Psi(t)|^2$, via

$$N(t)=|\Psi(t)|^2=|\Psi(0)|^2\exp(-\Gamma t)\quad,\quad \Gamma=\frac{-d\ln(N(t))}{dt} \qquad (10)$$

Such an exponential decay of the norm under the influence of the laser field is an approximation which is valid for the cases with constant ionization rate Γ. This equation, which is used routinely by researchers of the field, can thus be regarded as a definition for the ionization rate Γ.

The laser parameters used in our study are set to E_{0x}= 0.10676, ω=0.057, which are equivalent to 2.8×10^{14} W/cm^2 intensity and λ=800 nm wavelength. The time step is set to Δt=0.02 *au.* The rising time (ramp-on) and the ramp-off of the laser pulse are both selected to be 4 cycles. Duration of the full scale intensity is set to 10 cycles, thus the overall pulse duration is 18 cycles of the laser pulse.

3. RESULTS AND DISCUSSION

Variation of the probability density of the electron, $|\Psi(t)|^2$, with time for the ground state (n=1, $^2\Sigma$) of H_2^+ at several inter-nuclear distances (R) are calculated and demonstrated in Fig. 1. This figure shows that $|\Psi(t)|^2$ follows an exponential decay. This exponential variation is associated with relatively large background oscillations (the periodic appearance of the time durations over which the norm is relatively constant), i.e. with a steplike pattern caused by the oscillation of the laser field. In these time periods which happen around the maxima and minima of the electric field oscillations (and thus, the number of steps is equal to the number of oscillations of the laser field envelope), the ionization rate is nearly negligible and thus the wavefunction does not decay as rapidly as during the other time periods of the laser pulse.

As shown in Fig. 1, the time at which exponential decay in the norm of the wavefunction (and thus ionization) begins is different for different inter-nuclear separations. This behavior arises from the initial WP energy and the coulomb potential energy associated with each inter-nuclear distance. It can be seen from Fig. 1 that at some points of the laser pulse, the curves for different inter-nuclear separations larger than R=4.0 *au* intersect, showing that the slopes of the curves are different and change with time. This means that at these intersection points (times), the initial condition of the WP does not play a critical role in the determination of the ionization rate. The time-dependent behavior of the norm is sensitive to the initial state, and as the initial states are totally different, different behaviors for the norm and the corresponding instantaneous ionization rates are expected. This can be seen clearly, especially at the initial periods of the laser field. In other words, the results presented in Fig. 1 show that it is not possible to extrapolate the comparative ionization behavior of the WP's corresponding to different inter-nuclear distance R from the initial points of their interactions with the field.

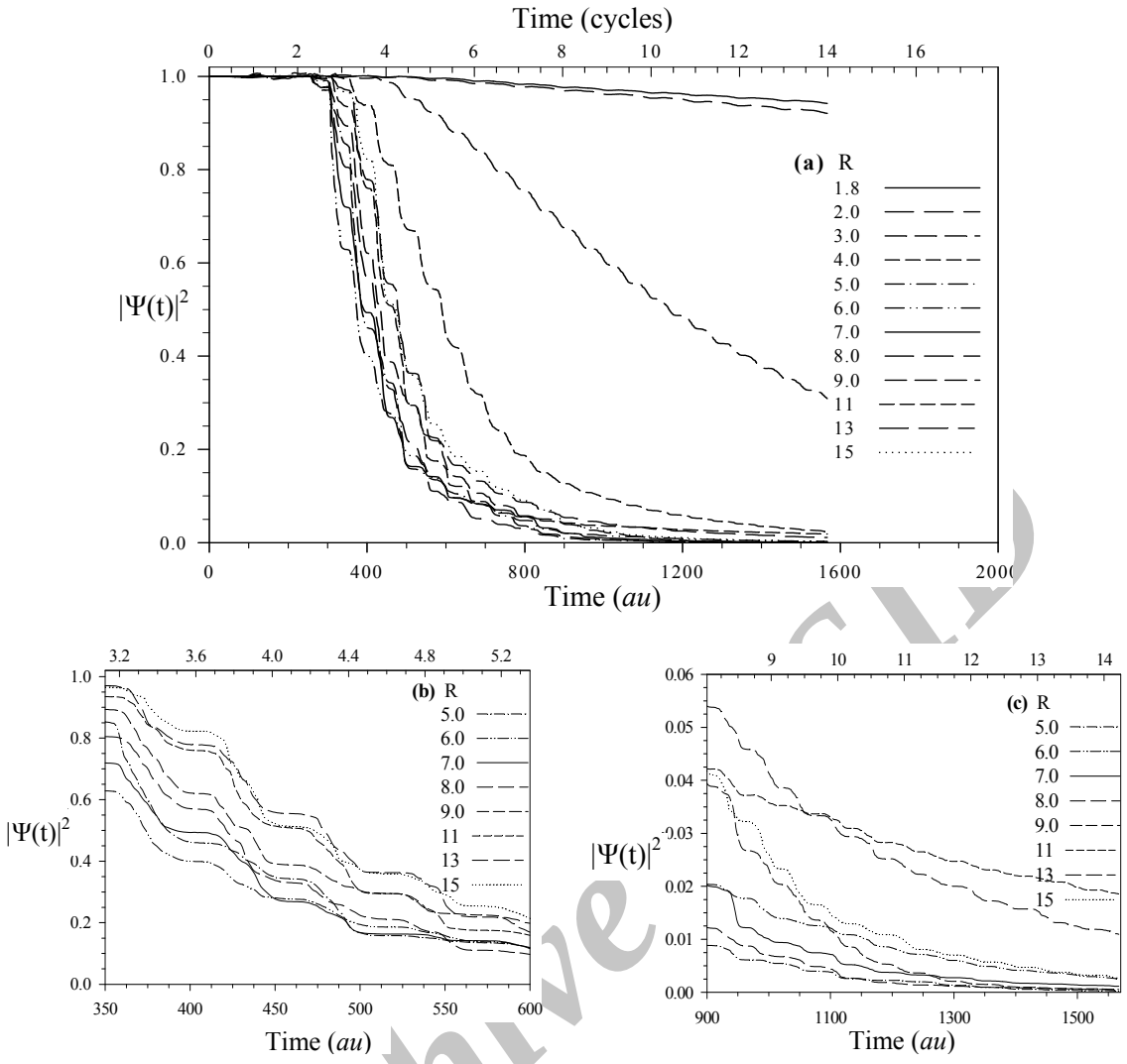

Fig. 1. Variation of the probability density or norm, $|\Psi(t)|^2$, of the H_2^+ 1-D model electron with time at different inter-nuclear distances obtained under the influence of a laser pulse of I=2.8×10^{14} W/cm^2 and λ=800 nm with the pulse shape given in Eq. (5). Curves are expanded in (b) and (c) for better resolution. The time axis atop the plots are given in terms of the cycles of the laser field

Figure 2 shows a comparison of the changes in the probability density of the electron with time for five different initial states of H_2^+ at two inter-nuclear distances 2.0 and 9.0 *au* (the corresponding *semi-log* plots are presented in Fig. 3). For the smaller inter-nuclear distance R = 2.0 *au*, the excited states show distinctly different behaviors from that of the ground state. Ponderomotive energy can account for this behavior, which is important in the higher excited states. The ponderomotive force is, at least partly, responsible for the decay of the norm at the longer times for the excited states. Similar to what was found for the time dependent norms of the ground state at different values of R (Fig. 1), here in Fig. 2, the curves for different initial states intersect. It can thus be said that the comparative ionization behavior of the WP's of different states evolve with time and cannot be extrapolated from the initial points of the interaction period. It is clear that at the inter-nuclear separation R = 2.0 *au*, the ground state and other excited states have different behaviors in the overall interaction time period. At the inter-nuclear separation R=9.0 *au*, the ground state and higher excited states have very similar behavior during the course of the laser field pulse.

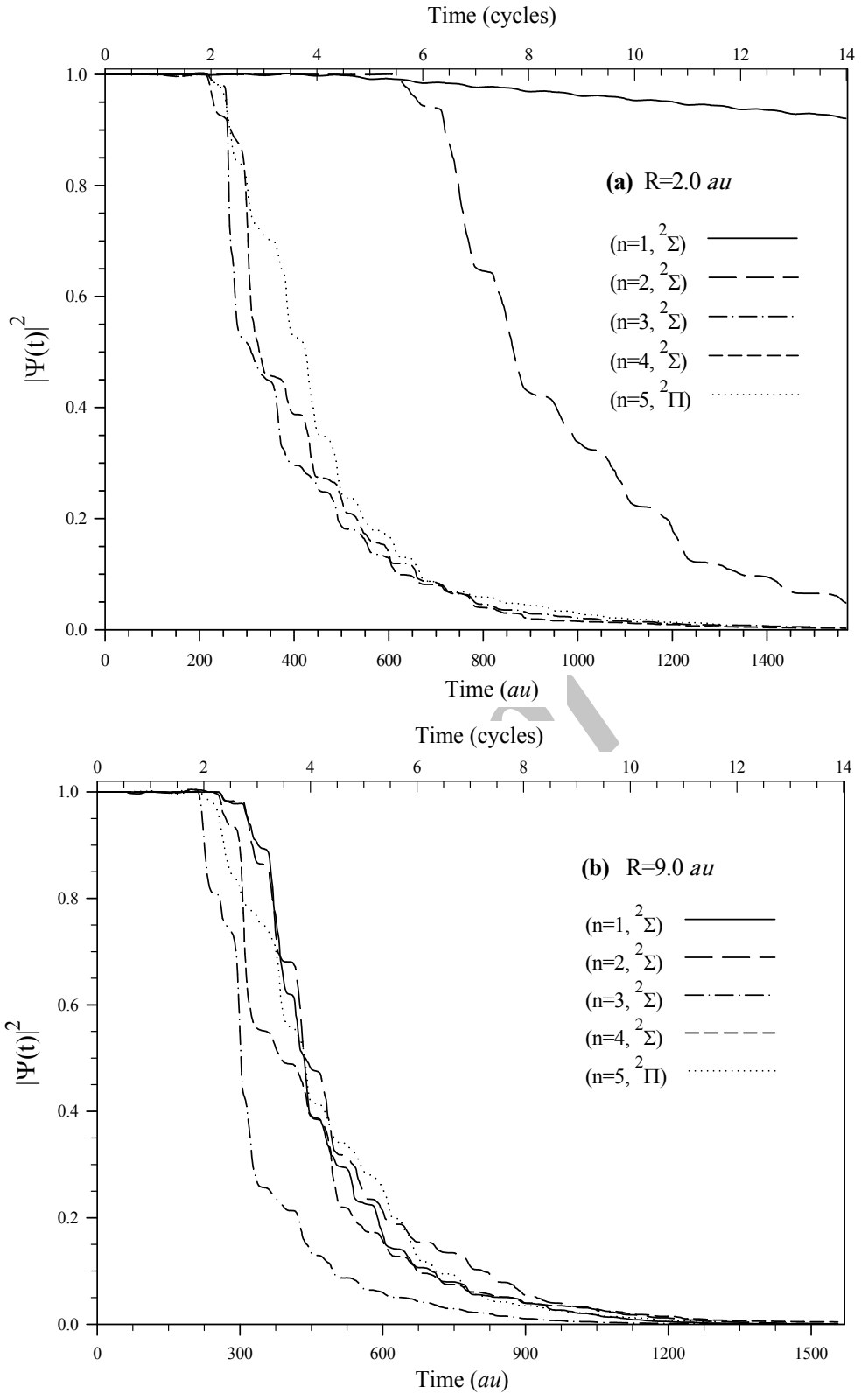

Fig. 2. Variations of the norm, $|\Psi(t)|^2$, of the H_2^+ 1-D model electron in the laser field of $I = 2.8\times10^{14}$ W/cm^2 and $\lambda = 800$ nm with the pulse shape given in Eq. (5) at different inter-nuclear distances (a) R=2 *au* and (b) R = 9 *au*

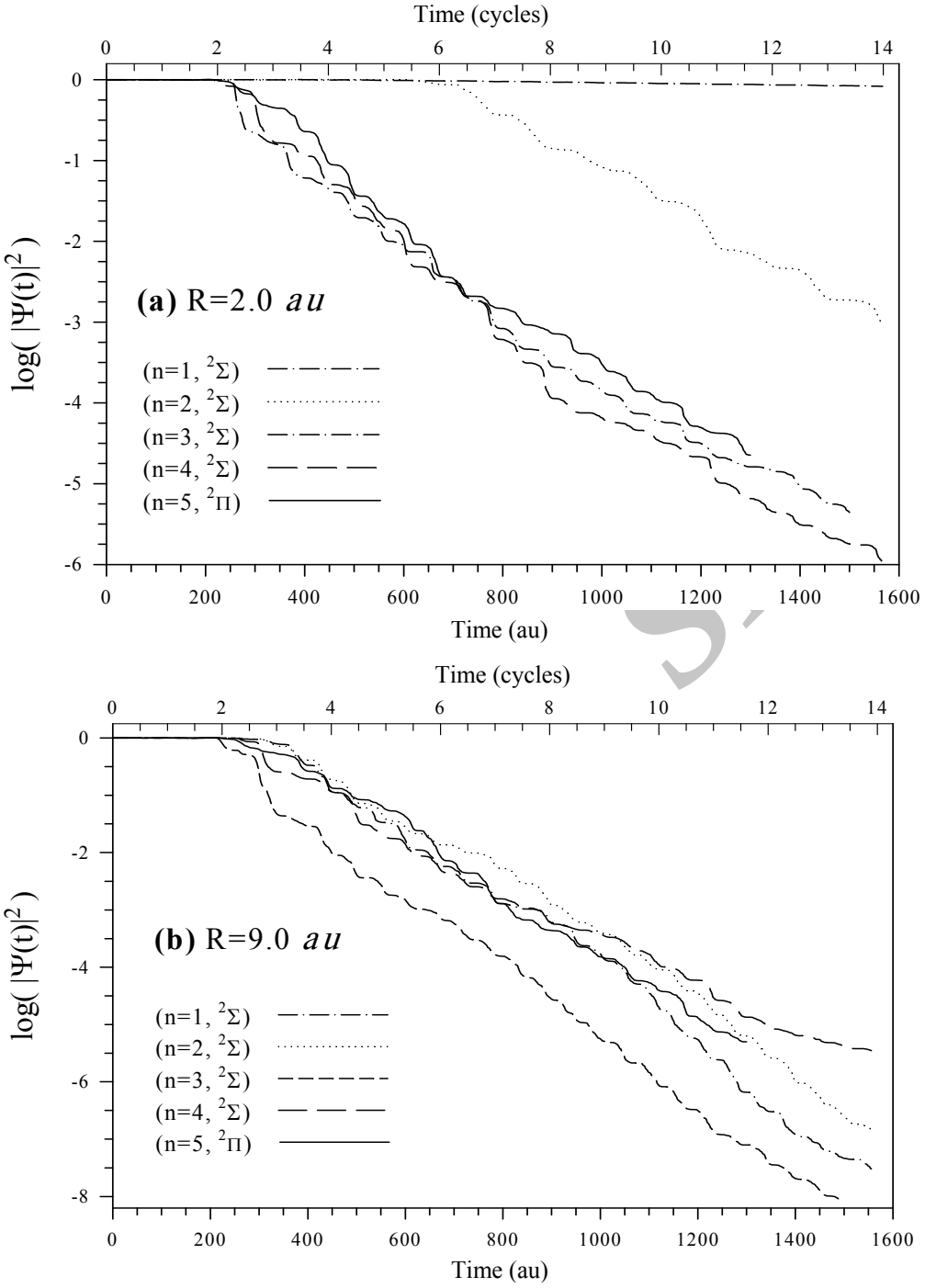

Fig. 3. Semi-log illustration of the time variations of the norm, $|\Psi(t)|^2$, of the 1-D H_2^+ system presented in Fig. 2

The correspondence between the variation of the probability density, $|\Psi(t)\square|^2$, of the ground state 1-D model of H_2^+ and the oscillations of the electric field of the laser pulse for inter-nuclear distance R = 9.0 *au* is illustrated in Fig. 4. It is clear from this figure that the rate of decay in the norm of the WP is small at the peaks and large in the rising or lowering regions of the laser field oscillations. This means that the ionization rate is larger in a short time period between each consecutive pair of maximum and minimum of the laser pulse electric field.

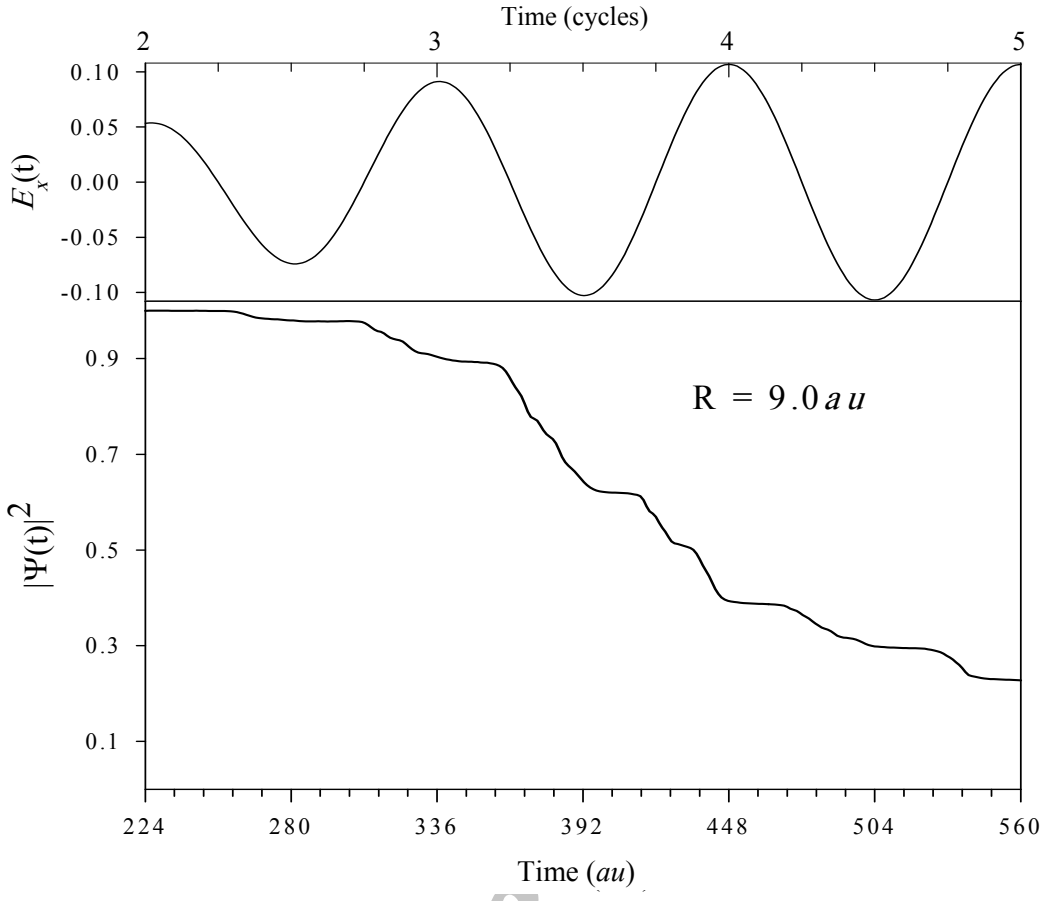

Fig. 4. Correlation between the variation of the norm of the 1-D model of the H_2^+ system at R=9.0 *au* and the oscillation of the electric field of the laser pulse during the time period from t=2 to t=5 cycles

Ionization rates of the 1-D H_2^+ in intense laser field as a function of inter-nuclear distance for five different initial states are calculated and shown in Fig. 5. The results obtained in this work for the ground state (n = 1, $^2\Sigma$) of the 1-D model of H_2^+ are very similar to that obtained in the previous studies for the 2-D and 3-D models [12, 13]. At small inter-nuclear distances ($R \leq 3.5$ *au*), ionization rates for the first (n = 2, $^2\Sigma$) to the fourth (n = 5, $^2\Pi$) excited states of the H_2^+ ion, projected onto a 1-D space, are larger than those of the ground state. The first peak of the ionization rate curve of the ground state (n = 1, $^2\Sigma$) appears at R = 4.5 *au*. Ionization rates of the second (n = 3, $^2\Sigma$) and the fourth (n = 5, $^2\Pi$) excited states also show a peak in this inter-nuclear separation. The ionization rates for different initial states show resonance enhancement at some inter-nuclear distances, which is in qualitative agreement with that obtained by a three-dimensional study on a two-state model, but with different sets of laser field parameters [24-26]. The results obtained for all five states show similar functional forms with inter-nuclear separations. The ionization behavior of the 1-D model of the H_2^+ system in each initial state at different inter-nuclear separations is different.

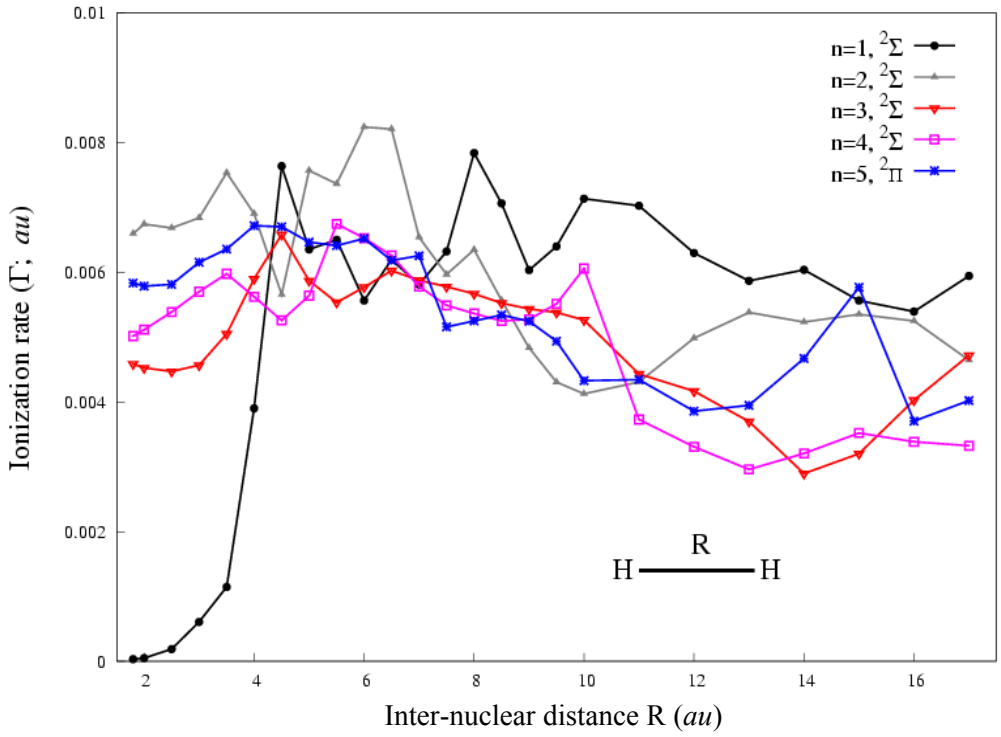

Fig. 5. Ionization rate, Γ, of the 1-D model of H_2^+ in intense laser field of I = 2.8×10^{14} W/cm^2 and λ = 800 nm as a function of inter-nuclear distance, R, calculated for five different initial states

The evolving electronic wavepacket can be represented in terms of a complete set of the H_2^+ field-free electronic states wavefunctions. For practical purposes, a limited number of basis functions is usually used. Figures 6-11 show the contributions from the five lowest field-free electronic wavefunctions (Φ_n ; n=1-5), to the time-dependent electronic wavepacket $\Psi(t)$ of the H_2^+ system calculated for three different cases starting from three different initial field-free electronic states at two different inter-nuclear separations, R = 2.5 and 9.0. Figs. 6-11 show clearly that at the smaller inter-nuclear separation R=2.5 (which is about the H_2^+ equilibrium distance), the time-dependent population pattern obtained for the $\Psi(0)=\Phi_1$ case (i.e. starting with the ground state wavefunction) is different from those obtained for other cases; with $\Psi(0) = \Phi_n$, n = 2-5. This is while at the larger inter-nuclear separation R = 9.0, the time-dependent population patterns obtained for different cases are similar. At R=2.5, if starting from $\Psi(0)=\Phi_1$ initial WP, variations of the populations of different states have almost fixed comparative phase shifts over the first two and the last two cycles of the laser pulse, while, if starting from $\Psi(0) = \Phi_{n\neq1}$ initial WPs, these variations have a relatively fixed phase shift only over the first two cycles of the laser pulse. At R = 9.0, no phase shift correlation could be established between the variations of different populations, regardless of the type of initial WP. Populations obtained for all cases at both inter-nuclear separations have a chaotic behavior, except for the $\Psi(0) = \Phi_1$ case at R = 2.5 which have well-behaved periodic patterns. This behavior is due to the fact that all of the H_2^+ field-free electronic states are non-bound except for the ground state at R = 2.5.

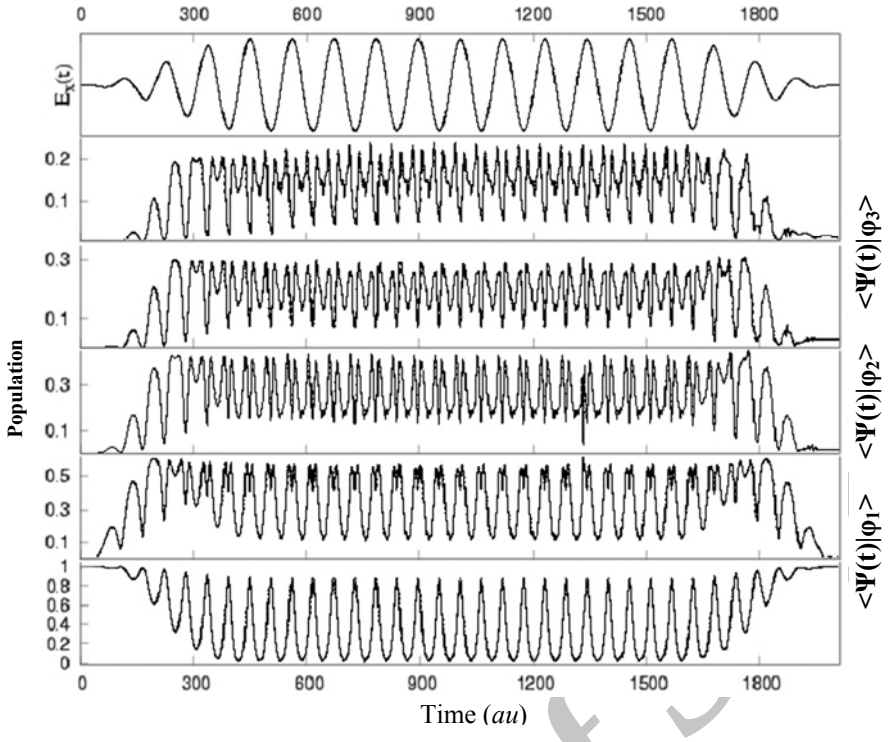

Fig. 6. Calculated contributions of the five lowest field-free electronic wavefunctions (Φ_n ; n=1-5), to the time-dependent electronic wavepacket $\Psi(t)$ of the 1-D model H_2^+ system at R = 2.5 *au* over the 18-cycle linearly polarized laser pulse with $\omega = 0.057$, $E_0 = 0.1067$ (corresponding to $I = 2.8\times10^{14}$ W/cm^2 and $\lambda = 800$ nm) starting from the $\Psi(0) = \Phi_1$ (ground state) as the initial WP

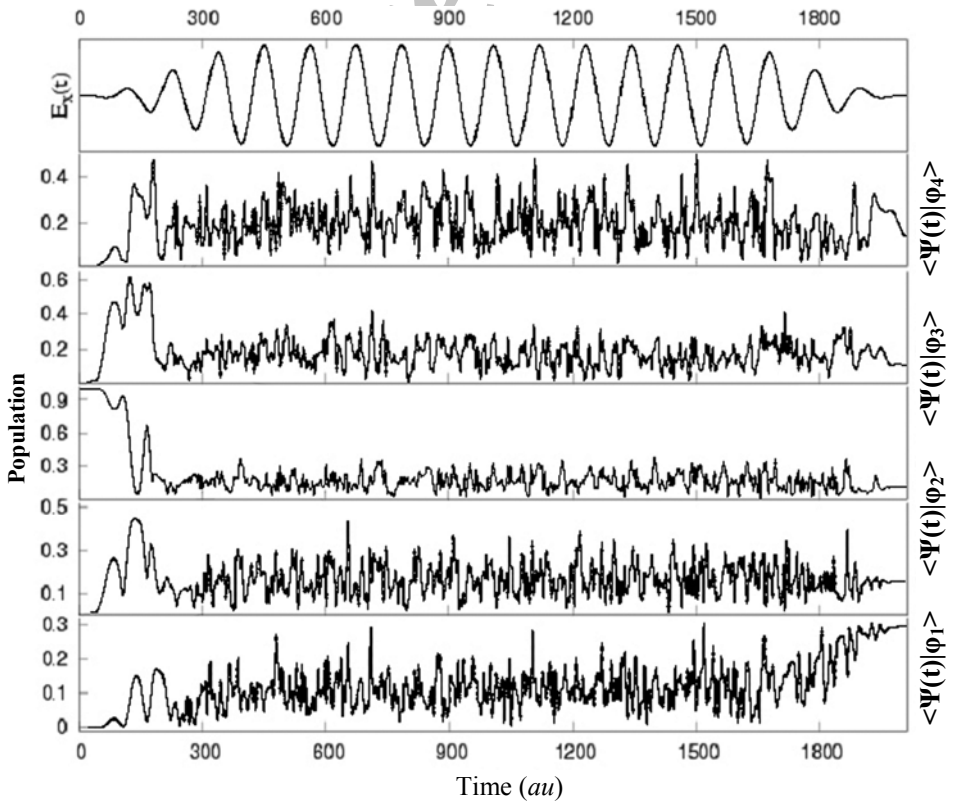

Fig. 7. The same as Fig. 6 at R = 2.5 *au*, but starting from $\Psi(0) = \Phi_3$ (the second excited state) as the initial WP

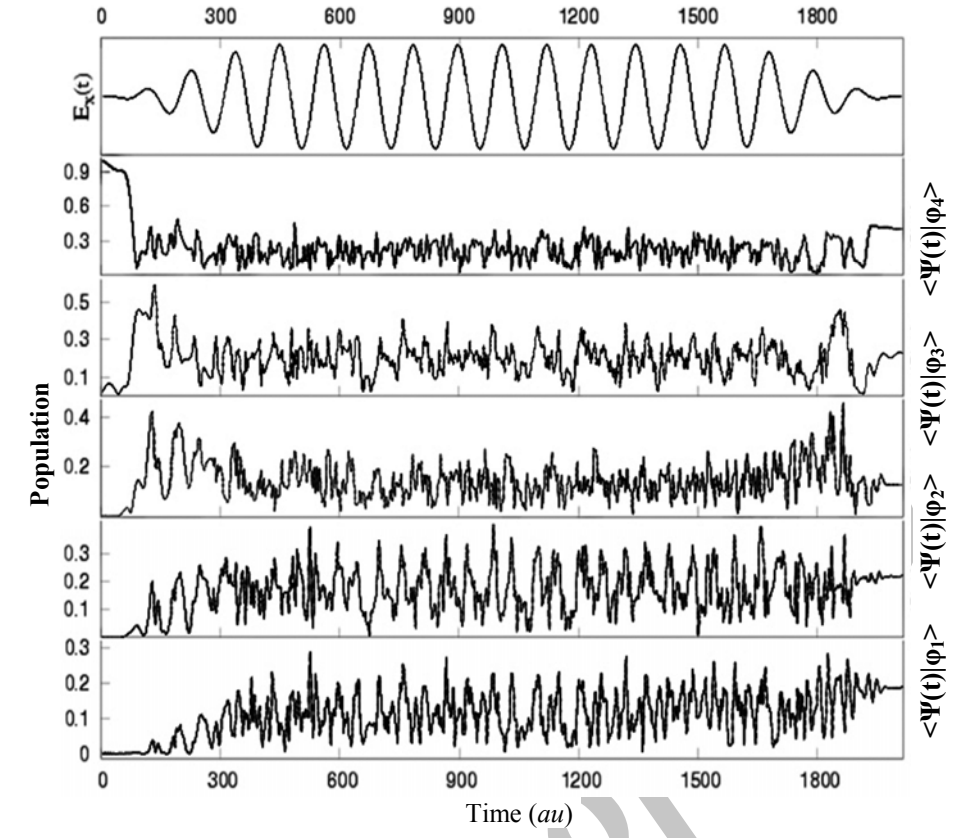

Fig. 8. The same as Fig. 6, at R = 2.5 *au*, but starting from $\Psi(0) = \Phi_5$ (the fourth excited state) as the initial WP

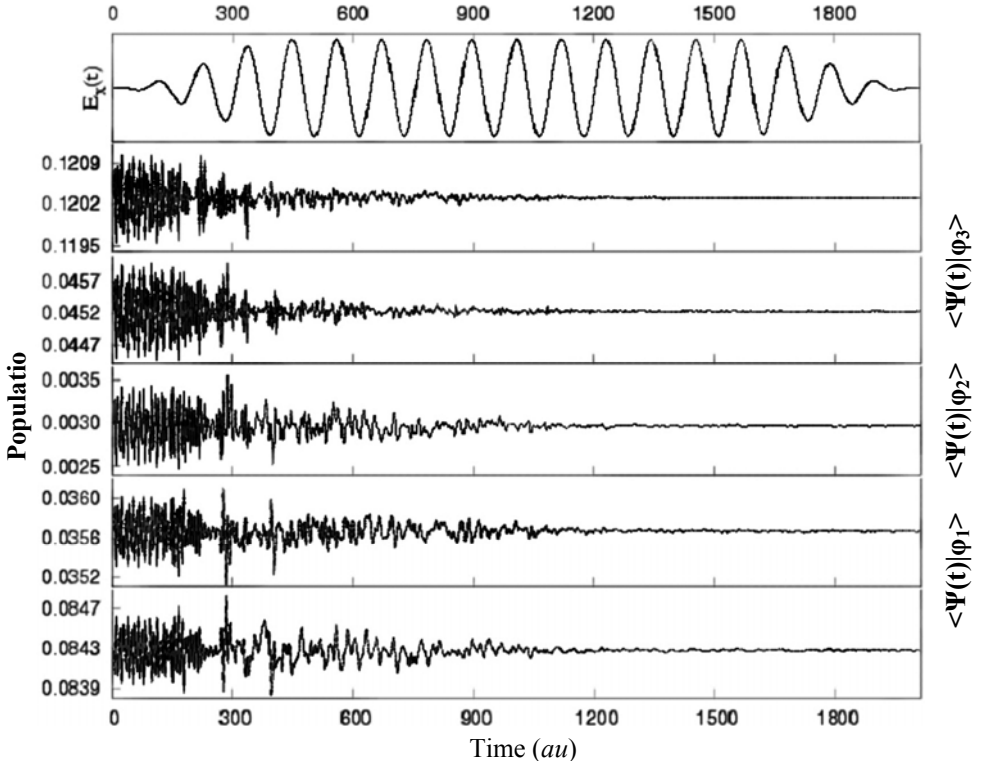

Fig. 9. The same as Fig. 6, but at R=9.0 *au* and starting from $\Psi(0) = \Phi_1$ (the ground state) as the initial WP

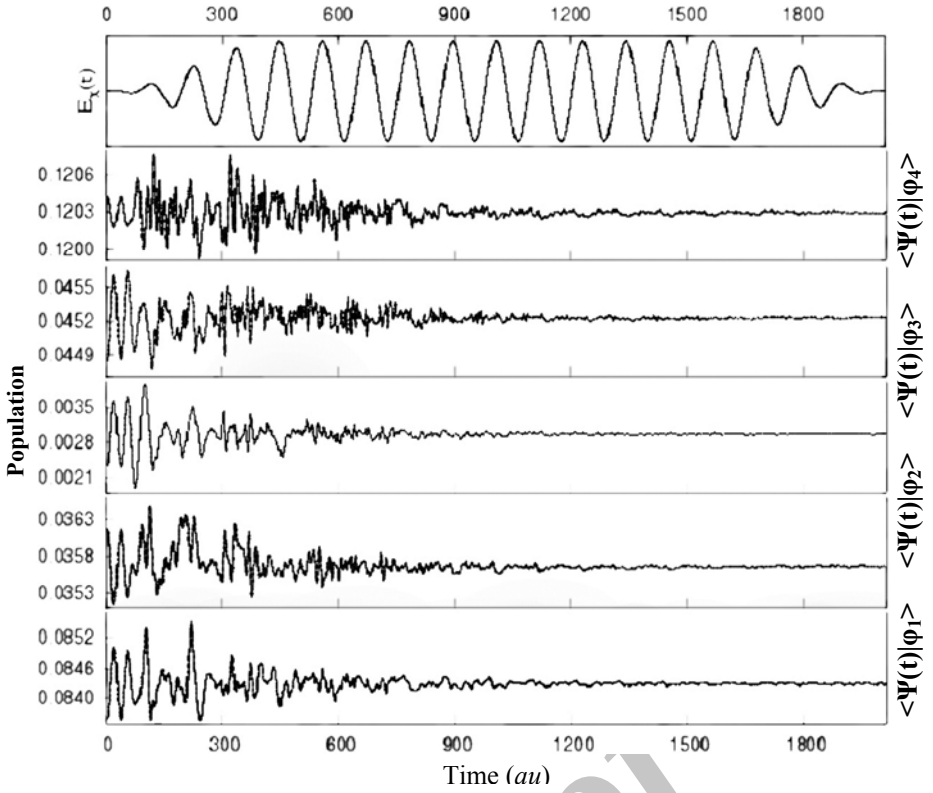

Fig. 10. The same as Fig. 9, at R = 9.0 *au*, but starting from $\Psi(0) = \Phi_3$ (the second excited state) as the initial WP

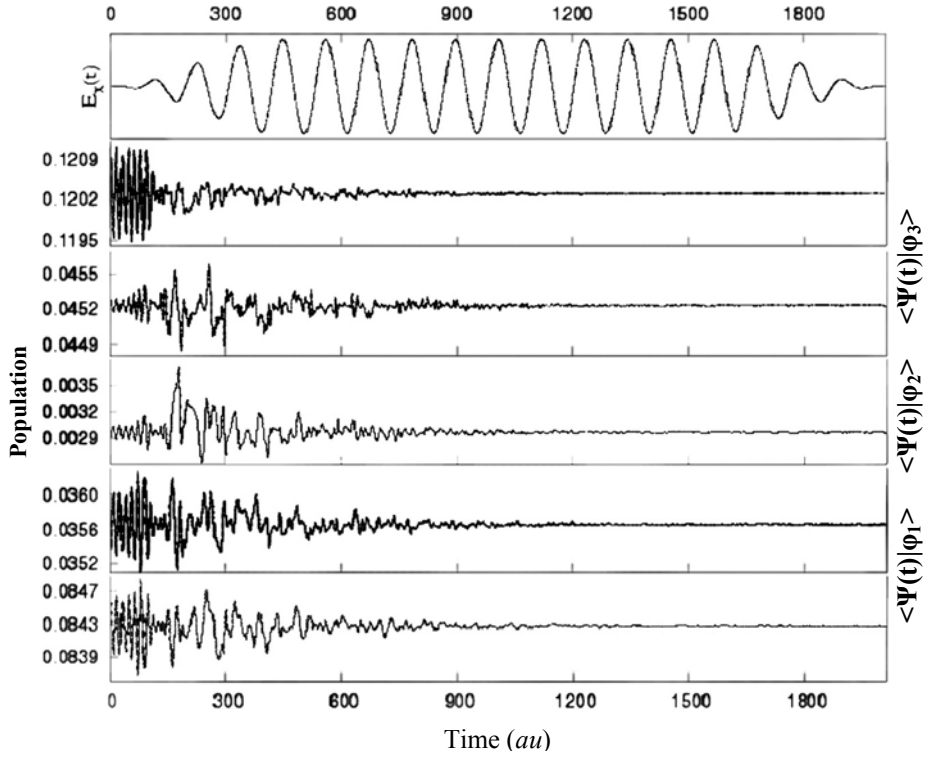

Fig. 11. The same as Fig. 9, at R = 9.0 *au*, but starting from $\Psi(0) = \Phi_5$ (the fourth excited state) as the initial WP

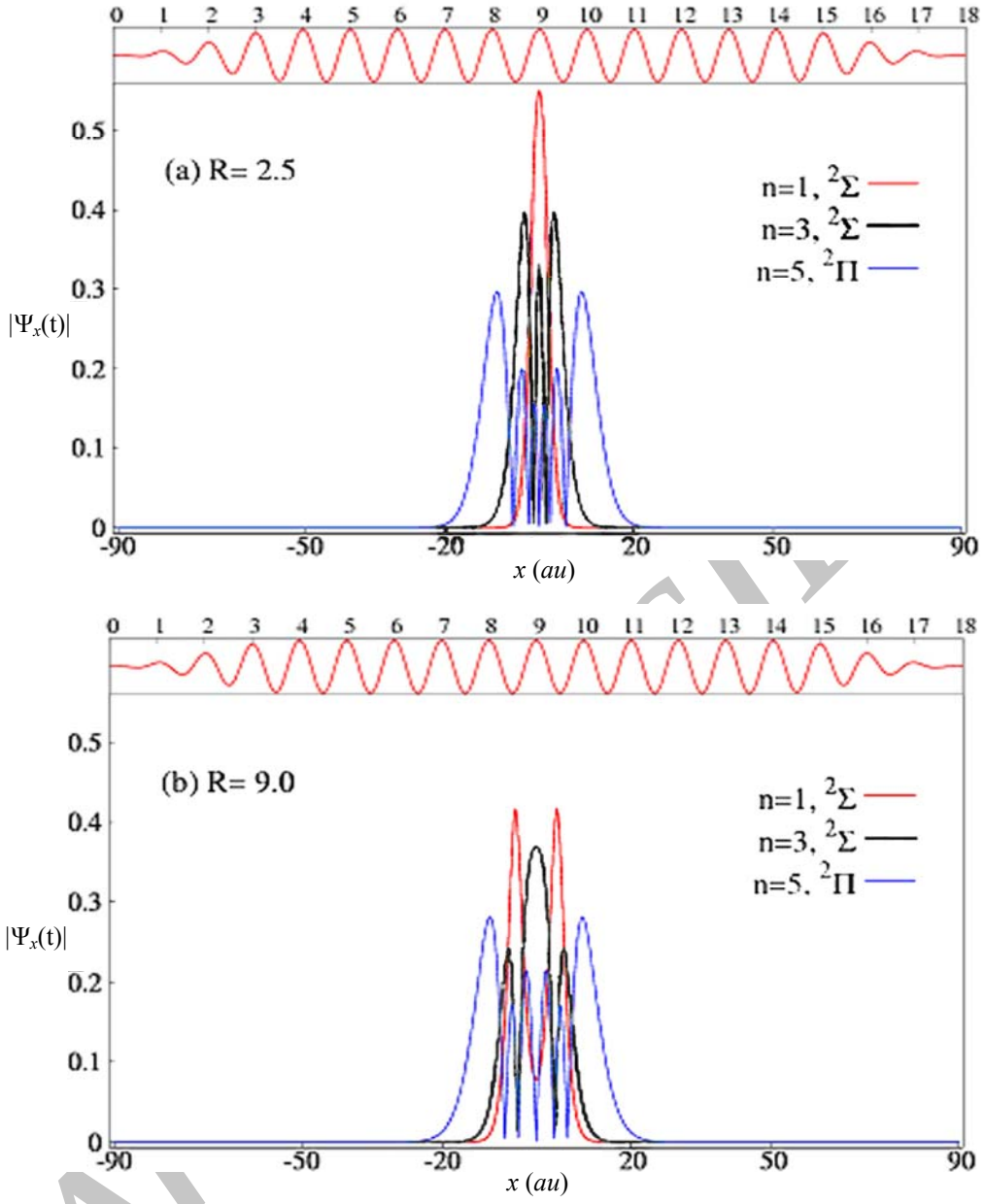

Fig. 12. Snapshots of the evolution of the 1-D H_2^+ molecular ion starting electron wavepacket from three different initial states in an 18-cycle linearly polarized laser pulse with $\omega = 0.057$, $E_0 = 0.1067$ (corresponding to $I = 2.8\times10^{14}$ W/cm^2 and $\lambda = 800$ nm) for (a) R = 2.5 *au* and (b) R = 9.0 *au*

For large values of R, the selected initial wavefunctions are so unstable that they immediately evolve (either via ionization or via the build-up in the other states) from unity to small values after the first few steps of calculations. This short period of time over which the norm takes distance from unity cannot be resolved in Figs. 9-11. For small values of R, however, the selected initial wavefunctions are relatively more stable and their norms survive longer to be observable in the time windows of Figs. 6-8.

Figure 12 shows slices of the animations illustrating the evolution process of the electron WP at two different inter-nuclear separations from three different initial states (Animations can be obtained from the authors). Animation of the WP evolution for R=2.5 *au*, Fig. 12(a), shows that in this inter-nuclear separation, the ground state (n=1, $^2\Sigma$) has a different behavior compared to the other two excited states (n=3, $^2\Sigma$) and (n=5, $^2\Pi$), although the behavior of the two excited states are similar. The animation of the WP evolution for R=9.0 *au,* Fig. 12(b), shows that the ground state and the other two excited states behave similarly. These animations show that most displacements of the WP correspond to the zero values of the

electric field oscillations. For the 1-D model used in this study, correlation of the time-dependent norm and the laser field oscillations is independent of the gauge; however, oscillation of the amplitude of the vector potential is shifted in the phase from the oscillations of the electric field by π/2.

For the 2-D and 3-D calculations, we would need to specify symmetry of the excited Σ states which can be viewed as the linear combinations of the *p*-orbitals or π-orbitals based on the treatments of the VB and MO theories, respectively. However, because of the projection of the wavefunctions onto the 1-D space, only σ_h symmetry survives, and all non-σ_h symmetries collapse and disappear. Therefore, the +/− symmetry of these excited Σ states does not contribute to the 1-D calculations. Therefore, the +/− label is omitted from these Σ states in this report.

4. CONCLUSION

We have studied and simulated the interaction picture of the linearly polarized laser pulse with a 1-D model of the H_2^+ molecular ion. The results obtained from this 1-D model are in qualitative agreement with the results reported previously for the 2-D or 3-D models. The ionization rates from different initial states showed that the behavior of the system in the ground state at small inter-nuclear separations (about equilibrium distance) is significantly different from those in the higher excited states. In the inter-nuclear separations larger than equilibrium distance, the ionization behaviors of all other initial states become similar. The ionization rates for different initial states show resonance enhancement at some inter-nuclear distances. Oscillations of the ionization rate curves with inter-nuclear separation at large values of R are significantly decreased and the curves are smoother.

Results of the present study showed that although the dimensionality of the model quantitatively affects the results considerably, it does not distort the qualitative picture of the ionization process of the H_2^+ system in the intense laser field ionization process. Therefore, it is worth trying to simulate the fragmentation process of the same model system in an intense laser field by releasing the nuclei and including the nuclear terms in the time-dependent Hamiltonian. Results of such a general 1-D model would then act as a benchmark for future test calculations on the H_2^+ 1-D model for a new laser field and system conditions.

Acknowledgment-Partial support of the University of Isfahan Research and Graduate offices as research facilities is greatly appreciated.

REFERENCES

1. Protopapas, M., Keitel, C. H. & Knight, P. L. (1997). Atomic physics with super-high intensity lasers. *Rep. Prog. Phys*., *60*, 389.
2. Ryabikin, M. Y. & Sergeev, A. M. (2000). Stabilization window and attosecond pulse train production at atom ionization in superintense laser field. *Optics Express*, *7*, 417.
3. Pfeifer, T., Walter, D., Gerber, G., Emelin, M. Y., Ryabikin, M. Y., Chernobrovtseva, M. D. & Sergeev, A. M. (2004). Transient enhancement of high-order harmonic generation in expanding molecules. *Phys. Rev. A*, *70*, 013805.
4. Rotenberg, B., Taïeb, R., Véniard, V. & Maquet, A. (2002). H_2^+ in intense laser field pulses: ionization versus dissociation within moving nucleus simulations. *J. Phys. B: At. Mol. Opt. Phys*., *35*, L397.
5. Alnaser, A. S., Osipov, T., Benis, E. P., Wech, A., Shan, B., Coke, C. L., Tong, X. M. & Lin, C. D. (2003). Rescattering double ionization of D_2 and H_2 by intense laser pulses. *Phys. Rev. Lett*., *91*, 163002.
6. Tong, X. M., Zhao, Z. X. & Lin, C. D. (2003). Probing molecular dynamics at attosecond resolution with femtosecond laser pulses. *Phys. Rev. Lett*., *91*, 233203.

7. Tong, X. M., Zhao, Z. X. & Lin, C. D. (2003). Correlation dynamics between electrons and ions in the fragmentation of D_2 molecules by short laser pulses. *Phys. Rev. A*, *68*, 043412.
8. Agostini, P., Fabre, F., Mainfray, G., Petite, G. & Rahman, N. (1979). Free-free transitions following six-photon ionization of xenon atoms. *Phys. Rev. Lett*., *42*, 1127.
9. Giusti-Suzor, A., He, X., Atabek, O. & Mies, F. H. (1990). Above-threshold dissociation of H_2^+ in intense laser fields. *Phys. Rev. Lett*., *64*, 515.
10. Brown, L. S. & Kibble, T. W. B. (1964). Interaction of intense laser beams with electrons. *Phys. Rev*., *133*, A705.
11. Freeman, R. R., Bucksbaum, P. H., Milchberg, H., Darack, S., Schumacher, D. & Geusic, M. E. (1987). Above-threshold ionization with subpicosecond laser pulses. *Phys. Rev. Lett*., *59*, 1092.
12. Vafaee, M. & Sabzyan, H. (2004). A detailed and precise study of the ionization rates of H_2^+ in intense laser fields. *J. Phys. B: At. Mol. Opt. Phys*., *37*, 4143.
13. Sabzyan, H. & Vafaee, M. (2005). Intensity dependence of the H_2^+ ionization rates in Ti:sapphire laser fields above the Coulomb-explosion threshold. *Phys. Rev. A*, *71*, 063404.
14. Bandrauk, A. D. & Lu, H. (2001). Moving adaptive grid methods for numerical solution of the time-dependent molecular Schrödinger equation in laser fields. *J. Chem. Phys*., *115*, 1670.
15. Bandrauk, A. D. & Shen, H. (1993). Exponential split operator methods for solving coupled time-dependent Schrödinger equations. *J. Chem. Phys*., *99*, 1185.
16. Geltman, S. (1977). Ionization of a model atom by a pulse of coherent radiation. *J. Phys. B: At. Mol. Opt. Phys*., *10*, 831.
17. Reed, V. C. & Burnett, K. (1992). Loss of harmonic generation in intense laser fields. *Phys. Rev. A*, *46*, 424.
18. Bandrauk, A. D. & Stephen, C. W. (1992). Coherence Phenomena in Atoms and Molecules in Laser Fields. *NATO ASI Series*, *B*: *Physics*, *287*.
19. De Raedt, H. & Michielsen, K. (1994). Algorithm to solve the time-dependent Schrödinger equation for a charged particle in an inhomogeneous magnetic field: Application to the Aharonov-Bohm effect. *Computers in Physics*, *8*, 600.
20. Natori, H. & Munehisa, T. (1997). Time-dependent Schrödinger equations with vector potentials - numerical calculations and visualizations. *J. Phys. Soc. Japan*, *66*, 351.
21. Sugino, O. & Miyamoto, Y. (1999). Density-functional approach to electron dynamics: Stable simulation under a self-consistent field. *Phys. Rev. B*, *59*, 2579.
22. Suzuki, M. (1990). Fractal decomposition of exponential operators with applications to many-body theories and Monte Carlo simulations. *Phys. Lett. A*, *146*, 319.
23. Mahapatra, S. & Sathyamurthy, N. (1997). Negative imaginary potentials in time-dependent quantum molecular scattering. *J. Chem. Soc., Faraday Trans*., *93*, 773.
24. Madsen, L. B. & Plummer, M. (1998). H_2^+ in intense laser fields: mechanisms for enhanced ionization in the multiphoton regime. *J. Phys. B: At. Mol. Opt. Phys*., *31*, 87.
25. Chu, X. & Chu, S. I. (2000). Complex-scaling generalized pseudospectral method for quasienergy resonance states in two-center systems: Application to the Floquet study of charge resonance enhanced multiphoton ionization of molecular ions in intense low-frequency laser fields. *Phys. Rev. A*, *63*, 013414.
26. Telnov, D. A. & Chu, S. I. (2005). Ab initio study of high-order harmonic generation of H_2^+ in intense laser fields: Time-dependent non-Hermitian Floquet approach. *Phys. Rev. A*, *71*, 013408.

Iranian Journal of Science & Technology, Transaction A, Vol. 33, No. A1
Printed in the Islamic Republic of Iran, 2009

IONIZATION OF A 1-D MODEL OF H_2^+ FROM DIFFERENT STATES IN INTENSE LASER FIELD*

H. SABZYAN** AND H. EBADI

Department of Chemistry, University of Isfahan, Isfahan 81746-73441, I. R. Iran
Email: sabzyan@sci.ui.ac.ir

یونش مدل یک بعدی H_2^+ از سطوح مختلف در میدان لیزر شدید

ح. سبزیان و ح. عبادی

گروه شیمی ،دانشگاه اصفهان، اصفهان، جمهوری اسلامی ایران

چکیده: معادله وابسته‌به‌زمان شرودینگر برای مدل یک‌بعدی یون مولکولی H_2^+ در میدان لیزر به شدت قطبیده در امتداد محور مولکول به روش عددی حل شده است. تحول زمانی بسته موج الکترونی در فواصل بین‌هسته‌ای معین و ثابت شبیه‌سازی و بررسی شده است. نتایج بدست‌آمده برای سرعت یونش از حالت پایه H_2^+ با نتایج گزارش‌شده برای مدلهای دوبعدی و سه‌بعدی تطابق کیفی خوبی نشان می‌دهد. در سرعت و جزئیات پدیده یونش از حالت برانگیخته، نقش حرکت پاندروموتیو مشهود است. به غیر از یونش از حالت پایه و در فواصل بین‌هسته‌ای تعادلی، فرآیند یونش بیشتر از راه سازوکار ورای آستانه رخ می‌دهد. سرعتهای یونش محاسبه‌شده نشان می‌دهد که برای فواصل بین‌هسته‌ای بزرگتر از ٤ واحد اتمی، فرآیند یونش از راه تشدید با حالتهای برانگیخته تقویت می‌شود.

*Received by the editor May 22, 2007 and in final revised form November 2, 2009
**Corresponding author